

## Electron capture and elastic scattering in high-energy $D^+ + D(1s)$ collisions

Y N Tiwari

Department of Physics, North-Eastern Hill University

Shillong-793022, Meghalaya (India)

yntiwari@gmail.com

### Abstract

Elastic scattering and electron capture cross-sections in the centre of mass system for collisions of deuteron with deuterium atoms have been calculated for the energy range from 5keV to 5MeV in the frame work of Coulomb-projected Born approximation. Differential cross-sections sections have been calculated in scattering angle range from 0-4 mrad at different deuteron incident energies.

**Key Words:** Elastic scattering, electron capture, Coulomb-projected Born approximation.

### Introduction

The studies of deuteron-deuterium collisions are of great significant in Physics as deuterium plays an important role in addressing several fundamental questions in astrophysics. The deuterium abundance is very important constituent for models of big-bang nucleosynthesis. Primordial D/H measurements provide the most sensitive probe of the baryon to photon density ratio  $\Upsilon$ . This, in combination with the cosmic microwave background measurement of the photon density, can be used to determine the cosmological baryon density (Burles and Tytler 1998, Lemoine et al 1999 and Tytler et al 1999). The study of deuterium may also be important in the formation of structure in the post recombination era of the early universe. The deuterated hydrogen molecule (HD) is the second most abundant molecule after  $H_2$  predicted to be produced in the combination of the universe (Lepp and Shull, 1984). Cooling radiation from it may play a very vital role in the formation of the first collapsing objects (Dalgarno *et al.*, 1973). Finally, as the universe evolves, deuterium slowly destroyed in the star, where burned into  ${}^3_2\text{He}$ . Mapping the temporal variations in the D/H abundance ratio can cast light on the time history of star formation in different regions of cosmos (Tosi *et al.*, 1998). Kristic and Schultz (1999) have studied the slow collisions charge transfer of isotopes of hydrogen atom in the very low energy range 0.1-100eV. Many textbooks have elaborated on charge transfer processes (McDowell and Coleman, 1970; Bransden and McDowell, 1992 and Eichler, 2005).

We have employed the Coulomb-projected Born approximation to the problem of deuteron-deuterium collisions to calculate electron capture cross-sections. The Coulomb-projected Born approximation which is a first order high-energy approximation was first proposed (Geltman, 1971) in which the plane wave of final scattering channel is replaced by the Coulomb wave to take account of the interaction between the ions. This is the first time that electron capture cross-sections in the deuteron-deuterium collisions studied in such a high-energy range. We have used atomic units throughout this paper ( $e = m = \hbar = 4fV_0 = 1$ ) except the cross-sections which either expressed in units of  $f a_0^2$  or  $a_0^2$  ( $a_0$  being the radius of the first Borh's orbit)

### Theory

We have considered the electron capture reaction



The differential cross-sections for the process (1) can be written as

$$\frac{d\ddagger}{d\Omega} = \frac{\tilde{\gamma}_i \tilde{\gamma}_f k_f}{4f^2 k_i} |T_{if}|^2 \quad (2)$$

Where,

$$\tilde{\gamma}_i = \frac{m_p(m_T + 1)}{m_p + m_T + 1} \quad \text{and} \quad \tilde{\gamma}_f = \frac{m_T(m_p + 1)}{m_p + m_T + 1}$$

Where again,  $m_p$  = mass of projectile ion and  $m_T$  = mass of target atom



The transition matrix in CPB approximation  $T_{if}^{CPBA}$  from an initial state  $i$  to a final state  $f$  in the CB approximation for the process (1) are given by

$$T_{if}^{CPBA} = \int \Phi_f^* V_f^* \Phi_i d\vec{r} d\vec{R}_f \quad (3)$$

Where  $\Phi_i$  and  $\Phi_f$  are the wave functions for the process (1) in the initial and final channels respectively and are given by

$$\Phi_i = w_i(\vec{r}') E_i(\vec{R}_i) \quad \text{and} \quad (4)$$

$$\Phi_f = w_f(\vec{r}) E_f(\vec{R}) \quad (5)$$

Where again,

$$w_i(\vec{r}') = \frac{1}{\sqrt{f}} e^{-S r_i} = \text{wave function of the } D \text{-atom in its ground state in the initial channel } (S = 1)$$

$$\Phi_f(\vec{r}) = \frac{1}{\sqrt{f}} e^{-S r} = \text{wave function of the deuterium atom in } 1s \text{ state in the final channel } (S = 1)$$

$$\{i(\vec{R}_i) = e^{i\vec{k}_i \cdot \vec{R}_i} \text{ is a plane wave in the initial channel.}$$

$$\{f(\vec{R}_f) = e^{-f r / 2} \Gamma(1 - ir) e^{i\vec{k}_f \cdot \vec{R}_f} {}_1F_1(ir; -ik_f R_f - i\vec{k}_f \cdot \vec{R}_f)$$
 is Coulomb wave

Where  $\vec{k}_i$  and  $\vec{k}_f$  are the momentum vectors in the initial and final channels respectively.

$r = \frac{\vec{r}}{k_f}$  is the repulsive Coulomb parameter and  ${}_1F_1(ir; -ik_f R_f - i\vec{k}_f \cdot \vec{R}_f)$  is the confluent hyper-geometric function.

Now the transition matrix element given in equation (3) will be

$$T_{if}^{CPBA} = \int d\vec{r} d\vec{R}_f e^{i(\vec{k}_i \cdot \vec{R}_i - \vec{k}_f \cdot \vec{R}_f)} \frac{e^{-S r_i}}{\sqrt{f}} e^{-f r / 2} \Gamma(1 + ir) {}_1F_1(ir; -ik_f R_f - i\vec{k}_f \cdot \vec{R}_f) \times \left( -\frac{1}{r_i} \right) \frac{1}{\sqrt{f}} e^{-S r} \quad (6)$$

Expressions for transition matrix given in equation (6) can be evaluated following Tiwari (2008)

The total cross-sections are obtained by integrating the expressions for differential cross-sections given by equation (2) as

$$\dagger = 2f \int \frac{d\dagger}{d\Omega} \sin \theta d\theta \quad (7)$$

Gauss-Legendre quadrature formula was used to perform numerical calculations by taking proper care of convergence.

## Results and discussion

We have calculated the differential as well as total cross-sections and presented the results in the form of figures. Fig.1 describes the graph of differential cross-sections for energies 30 and 60 keV, drawn angle versus differential cross-sections, angles in milliradian from 0 to 4 mrad in the X-axis and differential cross-sections in the units of  $a_0^2 sr^{-1}$  in the Y-axis. We observe a pronounced dip at about 1 mrad. And then follow the same trend as for the curve of energy 30keV. 30keV curve is shown by solid line and 60keV curve by dashed(.....) line. In Fig.2, the curves were drawn for energies 100, 200 and 300keV, 100keV by solid (\_\_\_) line, 200keV by dashed line (----) and 300keV by dotted line (....). We observe smooth curve and have a tendency of polite dip at 100keV curve and very slight dips in 100 and 200keV. Fig.3 shows the curves of differential cross-sections at energies 900 and 1500 keV, where the solid line is for 900keV and dashed line for 1500keV. The dips have been found at both the energies at .6 and 1 mrad angles. While, Fig.4 gives the total cross-sections curve drawn energies (keV) versus  $f a_0^2$ . Energy in X-axis and  $f a_0^2$  on Y-axis. Sharp peak at about 20keV energy was found and then decreasing monotonically. Fig.5 also shows the total cross-sections graph drawn energy versus  $f a_0^2$  on X-axis and Y-axis respectively. The decrease of cross-section as the increase of energy was observed. In fig.6 also we drawn graph energy versus  $f a_0^2$  on X-axis and Y-axis respectively and similar trend has been observed as in the fig.5. In Fig.7, where as energy variation is from 540 to 750 keV, we have clearly observed a dip at 630 keV energy. Such type of dip has not been

Fig.1. Graph of differential cross-sections for energies 30 and 60 keV

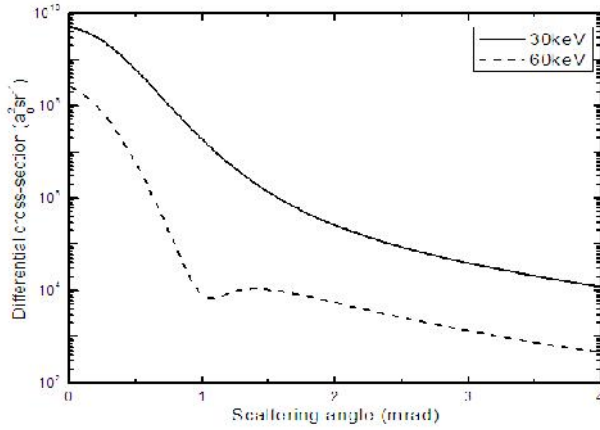


Fig.3. Graph of differential cross-sections for energies 900 and 1500 keV

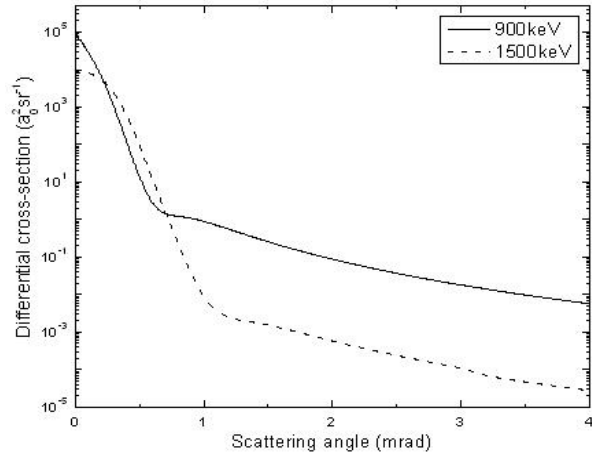


Fig.5. Graph of differential cross-sections

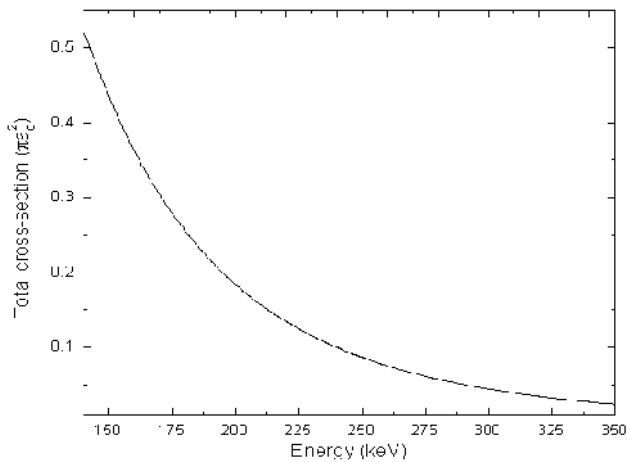


Fig.2. Graph of differential cross-sections for energies 100, 200 and 300 keV

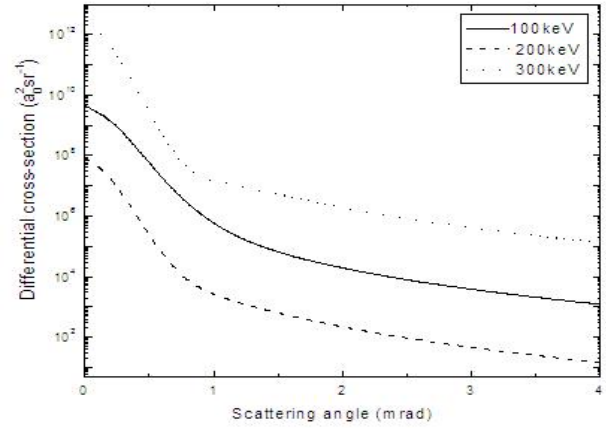


Fig.4. Graph of differential cross-sections

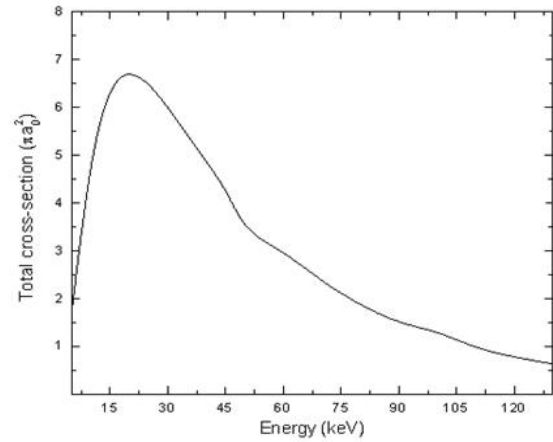


Fig.6. Graph of total cross sections

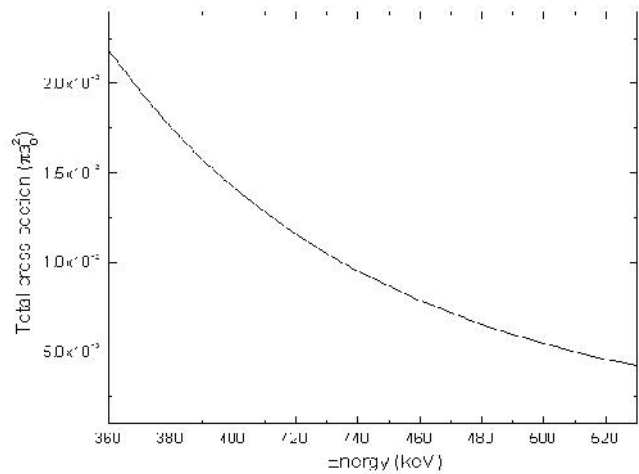


Fig.7 Graph of total cross sections

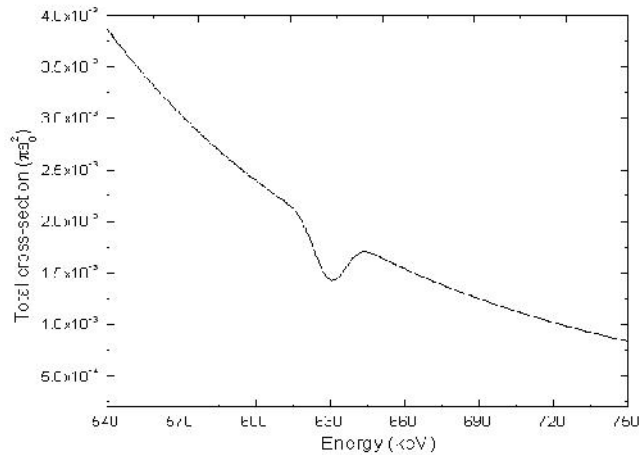
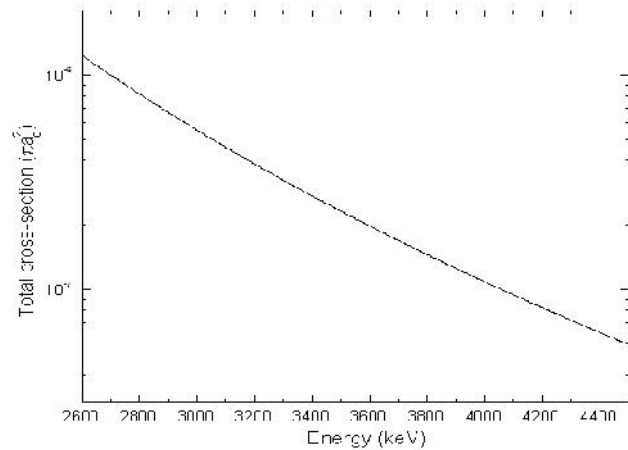


Fig.8. Graph of total cross sections



observed in the other graph of energy versus  $f a_0^2$  as we got a peak in Fig.4. After this dip the cross-section starts decreasing. In fig.8, we see the decrease of cross-section as increase of energy, which expected theoretically.

### Conclusion

Unfortunately, in such a range of energies in the deuteron-deuterium collisions, no other results are available either experimental or theoretical, we have not compared our results with other. The dip and peak found in the cross-section are interesting and further theoretical and experimental results are needed to compare our results.

### Reference

1. Bransden BH and McDowell MRC (1992), *Charge Exchange and the Theory of Ion-Atom Collisions*, Clarendon Press (Oxford).
2. Burles S and Tytler D (1998), The deuterium abundance toward Q1937-1009, *Astrophys.J*, 499,699-712.
3. Dalgarno A, Black JH, Weisheit JC (1973), Deuteron abundances, *Astrophys. Lett*, 14, 77.
4. Eichler J (2005), *Lectures on Ion-Atom Collisions (From non-relativistic to relativistic velocities)*, Elsevier.
5. Geltman S (1971), A high energy approximation: Proton-hydrogen charge transfer, *J. Phys. B*, 1288 -1298.
6. Krstic PS and Schultz DR (1999), Elastic scattering and Charge transfer in slow collisions: isotopes of  $H$  and  $H^+$  colliding with isotopes of  $H$  and with  $He$ , *J. Phys. B*, 32, 3485-3509.
7. Lemoine M, Audouze Jean, Jaffel Lotfi Ben, Feldman Paul, Ferlet Roger, H'ebnard Guillaume, Jenkins Edward B, Mallouris Christoforos, Moos Warren Sebach Kenneth, Sonneborn George, Vidal-Madjar Alfred and York Donald G (1999), Deuterium Abundances, *New Astronomy*, 4, 231-243.
8. Lepp S and Shull JM (1984) Molecules in the early universe, *Astrophysical J*, 280, 465-469.
9. McDowell MRC and Coleman JP (1970), *Introduction to the theory of Ion-Atom Collisions*, North-Holland, Amsterdam .
10. Tiwari YN (2008), Formation of H-atom in 2s excited state of proton-lithium and proton-sodium scattering, *J. Phys. Pramana*, 70(4):753-758.
11. Tosi M, Steigman G, Matteucci F and Chiappinni C (1998), Is High primordial deuterium consistent with galactic evolution? *Astrophysical J*, 498, 226-235.
12. Tytler D, O'Meara John M, Suzukin N and Lubin D (1999), Deuterium and the baryonic density of the universe, *Phys.Rep.* 333, 409-432.